Biogeosciences, 23, 4603–4621, 2026
https://doi.org/10.5194/bg-23-4603-2026

Biogeosciences Open Access EGU

Drought-induced soil carbon dynamics in subtropical forests: emergent divergence from model structures

Fengfeng Du[1], Lianjun Feng[1], Lingyan Zhou[2], Zhizhuang Gu[3], Yaqi Zhang[1], Zhenggang Du[1], and Xuhui Zhou[1]

[1]Northeast Asia ecosystem Carbon sink research Center (NACC), Key Laboratory of Sustainable Forest Ecosystem Management-Ministry of Education, School of Forestry, Northeast Forestry University, Harbin, 150040, China
[2]Shanghai Engineering Research Center of Sustainable Plant Innovation, Shanghai Botanical Garden, Shanghai, China
[3]Zhejiang Tiantong Forest Ecosystem National Observation and Research Station, School of Ecological and Environmental Sciences, East China Normal University, Shanghai, 200062, China

Correspondence: Zhenggang Du (zgdu@nefu.edu.cn)

Received: 15 October 2025 – Discussion started: 2 December 2025
Revised: 27 May 2026 – Accepted: 16 June 2026 – Published: 7 July 2026

Abstract. Accurately quantifying drought impacts on terrestrial carbon cycling is essential for advancing predictions of climate-carbon feedbacks. However, current biogeochemical models exhibit limited capability in simulating drought-induced transformations of soil organic carbon (SOC), particularly regarding microbial processes. Here, we conducted a systematic comparative evaluation of three prevailing SOC modeling structures, including conventional three-pool partitioning scheme (SM1), mineral and particulate- associated carbon partitioning scheme (SM2) and Michaelis-Menten regulated carbon-stabilization scheme (SM3), to elucidate their capacity in simulating soil carbon dynamics under decadal drought scenarios in a subtropical forest. We found divergent effects of drought in soil C input (SM1, 66 %; SM2, 10 %; SM3, −4 %) and mean residence time (MRT; SM1, −31 %; SM2, −14 %; SM3, 65 %), which lead to the predicted SOC substantial accumulation for both SM1 and SM3 (+39.5 % and +56.9 %, respectively) and moderate depletion (−6.1 %) for SM2. Drought leads to a decrease in microbial carbon and an increase in POC, while the responses of other carbon pools vary across different models. These findings highlight critical model structural dependencies in simulating drought-affected soil carbon dynamics and emphasize the necessity for models to integrate microbial-physicochemical interactions for improved climate-carbon coupling projections.

1 Introduction

Terrestrial ecosystems are facing increasing frequent stress from extreme drought which fundamentally alters plant-microbe-mineral interactions, serving as a key driver of carbon sequestration patterns (IPCC, 2023; Han et al., 2022; Choat et al., 2018; Hao and Singh, 2015). Initial drought exposure typically enhances soil organic carbon (SOC) stability via physicochemical protection mechanisms, such as reduced microbial decomposition from moisture limitation (Schimel, 2018), increased organo-mineral association due to soil contraction (Blankinship et al., 2016), and disrupted enzyme diffusion (Wu et al., 2025). However, plant-derived carbon inputs decline through productivity suppression driven by hydraulic failure (Choat et al., 2018) and carbon allocation shifts away from roots (Yin et al., 2021). Prolonged drought (e.g., >2 years) induces microbial adaptation strategies which may accelerate SOC loss (Barnard et al., 2013; Schimel, 2018). The shift toward filamentous fungal dominance enhances oxidative enzyme production, while necromass accumulation primes destabilization of mineral-associated carbon (Liang et al., 2020; Wang et al., 2024). However, predicting how terrestrial carbon storage responds to drought over decadal timescales remains a challenge, requiring the integration of long-term manipulative experiments with models capable of capturing drought-induced changes in plant-microbe-mineral interactions.

In most terrestrial ecosystem models, SOC is typically represented as discrete compartments defined by their turnover

times (Krinner et al., 2005; Lawrence et al., 2019). Early modeling approaches, such as the single-pool model proposed by Jenny (1941), treated SOC as a homogeneous system. Subsequent refinements led to the development of multi-pool frameworks. For example, Campbell (1978) categorized SOC into labile and stable organic matter. The TECO model further advanced this by partitioning SOC into three pools (fast, slow, and passive SOM) with different turnover rates (Xu et al., 2006; Du et al., 2017; Wan et al., 2025). Later developments incorporated greater complexity, such as separating recalcitrant fractions and accounting for physically protected organic matter, which decomposes more slowly than unprotected forms (Paul and Van Vee, 1978; Willard et al., 2024).

Theoretical advancements in soil organic matter (SOM) formation and decomposition improve the representation of SOC in land-surface and terrestrial ecosystem models (Basile-Doelsch et al., 2020; Si et al., 2024; Cotrufo and Lavallee, 2022; Sokol et al., 2019). Measured SOC fractions, such as particulate organic carbon (POC), mineral-associated organic carbon (MAOC) and dissolved organic carbon (DOC), have been proposed to link conceptual SOC pools (Lee and Rossel, 2020). POC is typically considered as fragments of plant residues with a particle size $> 53\,\mu m$, and it is more susceptible to external environment changes (Cotrufo et al., 2019; Benbi et al., 2014; Lugato et al., 2022). MAOC generally consists of microbial and plant-derived organo-mineral complexes rich in nutrients, typically $< 53\,\mu m$, while also being associated with minerals and embedded in soil aggregates (Si et al., 2024; Hansen et al., 2024; Villarino et al., 2021). Some studies have revealed that models constrained by measurable SOC pools can provide more accurate estimation of model parameters thereby more accurate projections of SOC dynamics (Guo et al., 2022; Tao et al., 2024; Abramoff et al., 2022). Dissolved organic carbon (DOC), derived from living roots or transformed from recalcitrant macromolecular organic matter, is approximately 2 to 3 times more efficient than litter in forming SOM (Sokol et al., 2019; Cotrufo et al., 2013). Moreover, the adsorption and desorption processes of DOC represent a key link in SOC decomposition (Camino-Serrano et al., 2018; Wu et al., 2014). Consequently, incorporating DOC and its interaction with SOC into models represents a crucial advance.

Soil organic matter decomposition is a stepwise process in which microbes secrete extracellular enzymes to catalyze the substrate, converting SOM into assimilable subunits (Caldwell, 2005; Szejgis et al., 2024). Extensive manipulative experiments reveal that short-term drought limits microbial activities and substrate decomposition rates by inducing osmotic stress and constraining substrate diffusion (Honeker et al., 2024; Citerne et al., 2021). In contrast, long-term drought alters microbial community structure and carbon utilization patterns (Hueso et al., 2012; Preece et al., 2019; Wang et al., 2024). As catalysts of decomposition, microbial enzyme activities are impacted by drought (Sardans and Peñuelas, 2010; Stursová et al., 2012; Wu et al., 2025). For example, drought significantly reduces the activities of β-glucosidase, acid phosphatase and polyphenol oxidase, although certain oxidases remain unaffected by soil moisture (Su et al., 2020a; Allison, 2023; Ficken and Warren, 2019). In recent years, microbial models, which focus on the process of microbial decomposition, have become increasingly incorporated in process-based ecological models (Moorhead and Sinsabaugh, 2006; Lawrence et al., 2009; Allison et al., 2010; Huang et al., 2018).

Despite these advancements, a critical knowledge gap remains: how structural uncertainty, fundamentally different assumptions about carbon stabilization, leads to divergent projections of SOC response to decadal drought which refers to continuously reduced approximately 70 % of natural rainfall sustained for over a decade (Su et al., 2020a). Traditional three-pool models feature conceptually unmeasurable carbon pools, and predictions of SOC rely solely on parameterization of total SOC (Guo et al., 2022), which obscures the responses of different carbon fractions (POC, MAOC, DOC) to drought and may lead to substantial errors in long-term projections. Furthermore, current models rarely explicitly represent the direct regulation of SOC by specific microbial enzymes and the effects of prolonged drought (Luo et al., 2020; Knorr et al., 2005; Eastman et al., 2024). Emerging frameworks that incorporate measurable fractions or explicit microbial enzyme kinetics (Michaelis-Menten dynamics) offer the potential to mechanistically represent the processes. However, these approaches differ fundamentally in their representation of carbon stabilization and decomposition, and no systematic evaluation has compared their performance against long-term drought experimental data. Such a comparison is essential, as the choice of model structure may not only influence predictive accuracy but also shape our mechanistic understanding of whether drought induces SOC loss or stabilization over decadal timescales.

In this study, we evaluate three SOC modeling schemes with increasing complexity, including conventional three-pool partitioning scheme (SM1), mineral and particulate- associated carbon partitioning scheme (SM2) and Michaelis-Menten regulated carbon-stabilization scheme (SM3). Using observational data from long-term drought experiments, we assess their validity and predictive performance. Our study addresses two key questions: (1) how does decadal drought affect SOC storage in subtropical forests? (2) do different model structures yield consistent drought impacts on SOC projections?

2 Materials and methods

2.1 Site description and data source

The Zhejiang Tiantong Forest Ecosystem National Field Scientific Observation and Research Station (28°48′ N,

121°47′ E, 163 m a.s.l.) is located in Ningbo, Zhejiang Province. The site has a typical mid-subtropical monsoon climate with relatively distinct seasons. Summers are generally mild and rainy, while winters are dry with little precipitation. The annual average temperature in the study area is approximately 16.2 °C. The annual average precipitation and evaporation are 1384 and 1320 mm, respectively, and the relative air humidity can reach 85 %. The predominant soil type in the site is red-yellow soil and soil parent materials are mainly weathered products of some granite and sedimentary rocks. The soil texture consists of sand (6.8 %), silt (55.5 %), and clay (37.7 %), with a pH ranging from about 4.4 to 5.1 (Gao et al., 2014). The vegetation type in the study area is typical subtropical evergreen broad-leaved forest, with secondary forests being the main vegetation type. The forest stocking density is approximately 3400 trees hm^{-2}. The drought experiment was established in July 2013, which is composed of three experimental plots with similar terrain, vegetation type and stand condition (Su et al., 2020b).

The forcing datasets used in this study span from 2014 to 2022, including photosynthetically active radiation (PAR), leaf area index (LAI), air temperature (T_a), relative humidity of air (RH), soil temperature (T_s) and moisture content of soil (SWC). These data were mainly measured by the station meteorological observation device. The above-ground biomass data of plants were mainly estimated by allometric growth equation. The C content of litter was determined by potassium dichromate oxidation method. Soil total organic carbon and its physical and chemical properties were measured by elemental analyzer. Microbial biomass carbon was determined by chloroform fumigation. DOC was determined by hot water extraction and element analyzer (Zhou et al., 2013). Soil enzyme activities were determined by microplate enzyme assay (Saiya-Cork et al., 2002; Su et al., 2020b) and was expressed by substrate conversion per gram of dry soil per hour. The soil respiration rate was measured using the *LI-COR 8100 portable system* (LI-COR. Inc., Lincoln, NE, USA) between 09:00 a.m. and 01:00 p.m. LT (local time) on 1–2 sunny days per month, and accumulated the data on daily scale.

2.2 Model description

All three soil models are coupled to a common vegetation submodule (Fig. 1). The vegetation model simulates photosynthesis and the flow of GPP within vegetation carbon pools. The photosynthesis process is implemented using the FBEM model, which is driven by leaf area index, photosynthetically active radiation, air temperature, and air relative humidity, detailed information can be found in Wu et al. (2009). Vegetation is divided into three carbon pools: foliage, fine roots, and wood. A portion of GPP is returned to the atmosphere as respiration, while the remaining Net Primary Productivity (NPP) is allocated as a carbon source to the three vegetation carbon pools. Carbon transferred from these three vegetation pools is directed to two litter pools: metabolic litter and structural litter. The decomposed carbon from the litter pools serves as the source for soil carbon pools, which is then input into three soil modules. In this way, we ensure that the three soil modules share the same meteorological forcing data and SOC input, thereby facilitating a better analysis of differences arising from model structure, detailed descriptions can be found in Du et al. (2025). In SM1, SOC is divided into three pools, including (1) a microbial pool with fast turnover; (2) a slow (chemically protected) pool, and (3) a passive (physically protected) pool (Xu et al., 2006; Du et al., 2015). In SM2, SOC is divided into four pools (Si et al., 2024), including (1) a dissolved organic carbon pool (DOC), which is converted from organic matter with high molecular weight and difficult to decompose. Microbes can utilize DOC and release CO_2 (Allison et al., 2010; Lawrence et al., 2009); (2) a microbial pool; (3) a particulate organic carbon pool (POC), and (4) a mineral- associated organic carbon (MAOC). SM3 is an extension of SM2 that incorporates three enzyme components: β-1, 4-glucosidase (BG), polyphenol oxidase (PPO), and cellobiohydrolase (CBH). These three enzymes provide a parsimonious yet functionally representative set for capturing drought effects on SOC decomposition (Chen et al., 2018). BG and CBH are primarily involved in the depolymerization of cellulose and labile carbon compounds, while PPO is associated with the oxidation of more recalcitrant substrates such as lignin-like compounds (Su et al., 2020b). Together, these enzymes capture the rate-limiting steps of both labile and resistant carbon decomposition. Given that enzymes have a low carbon content and their inclusion a pool could lead to model overparameterization, we therefore assign them a catalysis role instead of considering them as carbon pools. In these three model schemes, SM1 and SM2 implicitly represent microbial activities, where the decomposition of SOM governed by linear, first-order dynamics. Soil C turnover times are defined by biome and pool-specific decay constants, which are modified by environmental scalars such as soil temperature and soil moisture availability (Du et al., 2017, 2025). In contrast, the SM3 adopted reverse Michaelis-Menten kinetics to explicitly represent the catalytic progress of microbial extracellular enzymes. The turnovers of DOC, POC and MAOC are depended on the size of both the donor (substrate) and the receiver (microbial biomass) pools. SM1 was expressed by the following equations:

$$\frac{dC_M}{dt} = I + C_S c_7 a_{67} + C_P c_8 a_{68} - C_M c_6 \quad (1)$$

$$\frac{dC_S}{dt} = I + C_M c_6 a_{76} - C_S c_7 \quad (2)$$

$$\frac{dC_P}{dt} = C_M c_6 a_{86} + C_S c_7 a_{87} - C_P c_8 \quad (3)$$

Where C_M, C_S, C_P represent the C content of microbe, slow SOM and passive SOM. I represents the C input from litters, c_6, c_7, c_8 represent the exit rate of C from microbes,

slow SOM and passive SOM, and a_{67}, a_{68}, a_{76}, a_{78} represent the allocation of slow SOM to microbes, passive SOM to microbes, microbes to slow SOM and passive SOM to slow SOM, respectively.

The soil C pools of SM2 were expressed as follows:

$$\frac{dC_{DOC}}{dt} = I + C_{POC}c_7a_{67} + C_{MAOC}c_9a_{69} - C_{DOC}c_6 \quad (4)$$

$$\frac{dC_{POC}}{dt} = I + C_M c_8 a_{78} - C_{POC}c_7 \quad (5)$$

$$\frac{dC_M}{dt} = C_{DOC}c_6a_{86} - C_M c_8 \quad (6)$$

$$\frac{dC_{MAOC}}{dt} = C_{POC}c_7a_{97} + C_M c_8 a_{98} - C_{MAOC}c_9 \quad (7)$$

Where C_{DOC}, C_{POC}, C_{MAOC} represent the C content of DOC, POC, MAOC. Parameters c_6, c_7, c_8, c_9 denote the exit rate of DOC, POC, microbes and MAOC, and a_{67}, a_{69}, a_{78}, a_{86}, a_{97}, a_{98} represent the allocation of POC to DOC, MAOC to DOC, microbes to POC, DOC to microbes, POC to MAOC and microbes to MAOC, respectively. SM3 was expressed by the following equations:

$$\begin{aligned}\frac{dC_{DOC}}{dt} &= I + a_{67}(V_{CBH.P} + V_{PPO.P} + V_{BG.P})C_{POC} \\ &\quad + a_{69}(V_{CBH.M} + V_{PPO.M} + V_{BG.M})C_{MAOC} \\ &\quad - \frac{V_{max.assim}C_M C_{DOC}}{KM_{assim} + C_{DOC}}\end{aligned} \quad (8)$$

$$\begin{aligned}\frac{dC_{POC}}{dt} &= I + C_M c_8 a_{78} \\ &\quad - (V_{CBH.P} + V_{PPO.P} + V_{BG.P})C_{POC}\end{aligned} \quad (9)$$

$$\frac{dC_M}{dt} = C_{DOC}c_6a_{86} - C_M c_8 \quad (10)$$

$$\begin{aligned}\frac{dC_{MAOC}}{dt} &= a_{97}(V_{CBH.P} + V_{PPO.P} + V_{BG.P})C_{POC} + a_{98}c_8C_M \\ &\quad - (V_{CBH.M} + V_{PPO.M} + V_{BG.M})C_{MAOC}\end{aligned} \quad (11)$$

Where $V_{max.assim}$ and KM_{assim} denote microbe maximum assimilation rate and half-saturation for assimilation. $V_{CBH.P}$, $V_{PPO.P}$, $V_{BG.P}$ represent catalytic rate of CBH, PPO, BG to POC. $V_{CBH.M}$, $V_{PPO.M}$, $V_{BG.M}$ represent catalytic rate of CBH, PPO, BG to MAOC.

$$V_{enzy.P} = \frac{V_{max.enzy}f_{enzy}C_M}{KM_{enzy} + C_{POC}} \quad (12)$$

$$V_{enzy.M} = \frac{V_{max.enzy}f_{enzy}C_M}{KM_{enzy} + C_{MAOC}} \quad (13)$$

Where $V_{max.enzy}$ represent the maximum reaction rate. KM_{enzy} represent half-saturation for reaction, f_{enzy} represent the C ratio of CBH, PPO, BG to microbes, respectively. The enzyme activities were calculated as following:

$$V_{enzy} = \frac{V_{max.enzy}f_{enzy}C_M C_{sub}}{KM_{enzy} + C_{sub}} \quad (14)$$

Where C_{sub} denotes the C content of the enzyme-catalyzed substrate contained within a soil block with an area of 1 m^2 and a depth of 10 cm, and it maintains a consistent ratio of enzyme to substrate as required for experimental measurements.

To quantify model uncertainty, we employed the MCMC data assimilation method (Xu et al., 2006) to invert model parameters (Table A1). Subsequently, 1000 sets of parameters were randomly sampled from the posterior distribution of each parameter to generate predictions (Fig. 3). The standard deviation of the 1000 simulation results for total organic carbon (TOC) in the year 2100 from each model was used to represent the magnitude of uncertainty arising from model parameters. The traceability analysis framework (Supplement) was used to evaluate changes in the simulated ecosystem C storage capacity. The effect of drought on C storage is calculated as follows:

$$\text{Drought Effect} = \frac{(C_{drought} - C_{ctr})}{C_{ctr}} \times 100\,\% \quad (15)$$

Where $C_{drought}$ represents the C content of drought, C_{ctr} represents the C content of control condition.

3 Results

3.1 Model validation

In this study, we used the Markov Chain Monte Carlo (MCMC) algorithm to constrain model parameters (Figs. 2 and A3). All schemes incorporate 8 vegetation-related parameters (Fig. A3). SM1 included 8 soil carbon-related parameters (Fig. 2), with 5 well-constrained under control conditions (c_7, a_{86}, a_{67}, a_{87}, a_{68}) and 5 under drought conditions (c_7, c_8, a_{76}, a_{86}, a_{68}). SM2 consisted 14 soil carbon-related parameters, with 7 well-constrained in the control scenario (c_9, c_{10}, a_{74}, a_{65}, a_{67}, a_{97}, a_{78}) and 9 in the drought scenario (c_9, c_{10}, a_{64}, a_{74}, a_{86}, a_{67}, a_{97}, a_{98}, a_{69}). SM3 had 11 well-constrained parameters under control conditions ($V_{max.assim}$, $V_{max.CBH}$, KM_{CBH}, f_{CBH}, f_{BG}, f_{PPO}, a_{64}, a_{74}, a_{75}, a_{97}, a_{78}) and 12 under drought conditions (c_6, $V_{max.assim}$, $V_{max.CBH}$, KM_{CBH}, KM_{BG}, $V_{max.PPO}$, KM_{PPO}, f_{BG}, f_{PPO}, a_{65}, a_{86}, a_{97}) in all 22 soil carbon-related parameters.

All three schemes calibrated by observations from the drought experimental which had overall good agreement (Figs. A1 and A2). The simulation of vegetation C (leaf, fine root, wood) and soil respiration exhibited high accuracy. The simulated MBC by SM1 was inferior to those simulated by SM2 and SM3, suggesting that incorporating measurable C pools can improve the accuracy of MBC simulation. By comparing the accuracy of POC and MAOC, we found that SM3 generally outperformed SM2, indicating that the incorporation of enzyme activities can enhance the simulation of the SOC fractions, particularly with respect to MAOC.

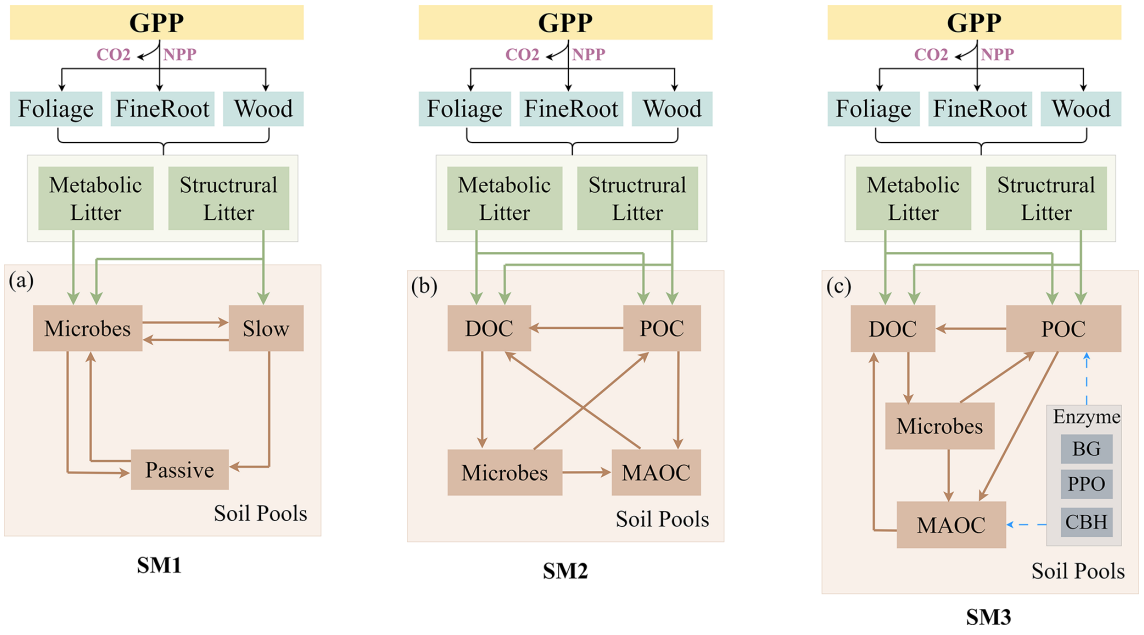

Figure 1. Conceptual diagram of the soil biogeochemical models with three schemes. **(a)** Conventional three-pool partitioning scheme (SM1), **(b)** mineral and particulate- associated carbon partitioning scheme (SM2), and **(c)** Michaelis-Menten regulated carbon-stabilization scheme (SM3). All pools (boxes) and fluxes (arrows) represent C process. BG, β-1, 4-glucosidase, PPO, polyphenol oxidase, CBH, cellobiohydrolase.

3.2 Carbon simulation and prediction by three model schemes

Carbon storage from 2023 to 2100 was predicted using three different model schemes. All models consistently indicated an increasing trend in vegetation C (VegC) and a decreasing trend in SOC under both control and drought conditions (Figs. 3 and A4). Specifically, under control conditions, SM1 simulated change rates of 260 % for VegC, −56.9 % for SOC and 188 % for total organic carbon (TOC). Under drought conditions, the corresponding rates were 223 %, −50.4 % and 159 %. SM2 projected growth rates of 263 % for VegC, −60.8 % for SOC and 179 % for TOC under control conditions, and 217 %, −55 % and 151 % under drought. For SM3, the simulated growth rates were 230 % for VegC, −88 % for SOC and 146 % for TOC in the control scenario, while under drought the values were 169 %, −55 % and 106 %, respectively.

The coefficient of variation (CV) of predicted TOC in 2100 across 1000 parameter sets was 0.12 for SM1, 0.15 for SM2, and 0.22 for SM3. Importantly, the difference between the highest and lowest median TOC predictions among the three models (SM1, 5.2, SM2, 4.1, SM3, 3.8 kg C m^{-2}) is approximately 2.5 times larger than the average within-model parametric uncertainty (mean SD, 0.6 kg C m^{-2}), demonstrating that model structural uncertainty dominates (Fig. 3j).

3.3 Drought effects on carbon storage

All three modeling schemes consistently indicated that drought reduced C content in MBC (SM1, −36.9 %; SM2, −56.9 %; SM3, −27.3 %), VegC (SM1, −16.8 %; SM2, −19.9 %; SM3, −25.4 %) and TOC (SM1, −15 %; SM2, −19.4 %; SM3, −24.4 %). However, the simulated responses of SOC to drought varied among the schemes (Fig. 4). SM1 predicted an increase in SOC under drought conditions (+39.5 %) compared to the control, driving by increases in both the slow (+13 %) and passive (+57 %) C pools. Similarly, SM3 projected a rise in SOC (+56.9 %), accompanied by increases in POC (+82.3 %), MAOC (+88.1 %), and DOC (+6.7 %). In contrast, SM2 simulated a decrease in SOC (−6.1 %), with reductions in DOC (−35.3 %) and MAOC (−3.7 %), through POC increased (+43.4 %).

By comparing the proportion of drought effects on each carbon pool simulated by each model to the total drought effects across the three models, it is apparent that different modeling schemes exhibit distinct sensitivities to drought (Fig. 4). Specifically, SM2 demonstrated greater sensitivity to drought effects on microbial biomass (−54 %) and DOC (−84 %) compared to SM3 (−18 % and +16 %, respectively). Conversely, SM3 showed higher sensitivity to drought-induced changes on POC (+82 %) and MAOC (+74 %) relative to SM2 (−26 % and +18 %, respectively).

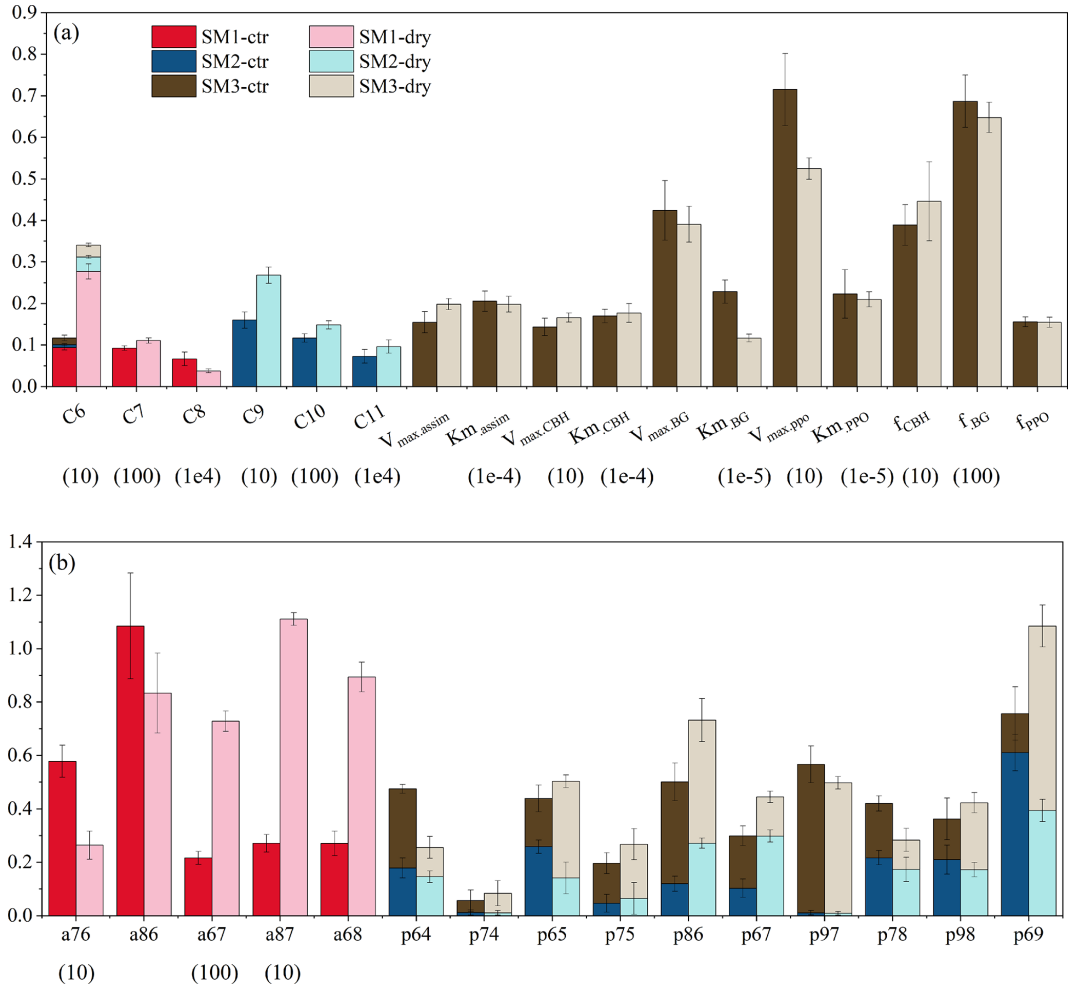

Figure 2. Maximum likelihood estimates (MLEs; or means for unconstrained parameters) of the target parameters under control and drought treatments across the three schemes. Error bars indicate standard deviations (SDs). Refer to Table A1 for parameter abbreviations and units.

3.4 Traceability analysis of drought effects

The traceability analysis revealed that both SM1 and SM3 simulated higher SOC under drought condition (SM1, 2.5 kg C m^{-2}; SM3, 1.2 kg C m^{-2}) compared to the control (SM1, 2.1 kg C m^{-2}; SM3, 0.8 kg C m^{-2}) at the end of forecast period (Fig. 5). In contrast, SM2 simulated lower SOC under drought (2.3 kg C m^{-2}) compared to the control (2.5 kg C m^{-2}). The increase of SOC in SM1 during drought was driven by higher soil carbon input (drought, 1.0 kg C m^{-2} yr^{-1}; control, 0.6 kg C m^{-2} yr^{-1}) (Fig. 4), while in SM3, it resulted from an extended soil carbon residence time (drought, 4.3 years; control, 2.6 years). However, SM2 simulated a reduction in soil carbon residence time under drought, leading to decreased SOC.

We further analyzed the C residence times of individual pools simulated by the three modeling schemes under both control and drought conditions (Fig. 4c). In SM1, drought increased the C residence time of passive SOM. For SM2, drought reduced the C residence time of microbes and increased that of MAOC. In SM3, drought resulted in a longer C residence time for MAOC.

4 Discussion

4.1 Response of ecosystem carbon dynamics to long-term drought

In this study, all three modeling schemes consistently indicate that drought leads to decrease in vegetation carbon, microbes carbon (Microbe C) and total organic carbon (TOC), while POC increases under drought conditions (Figs. 3, 4 and A4). These findings are consistent with multiple fields manipulated experiments (Zhou et al., 2020; Pennisi, 2022; Schwalm et al., 2017). During drought, plants undergo physiologically adjustments and shifts in community structure in accordance with species-specific water use strategies to prevent excessive water loss (Rowland et al., 2023). These re-

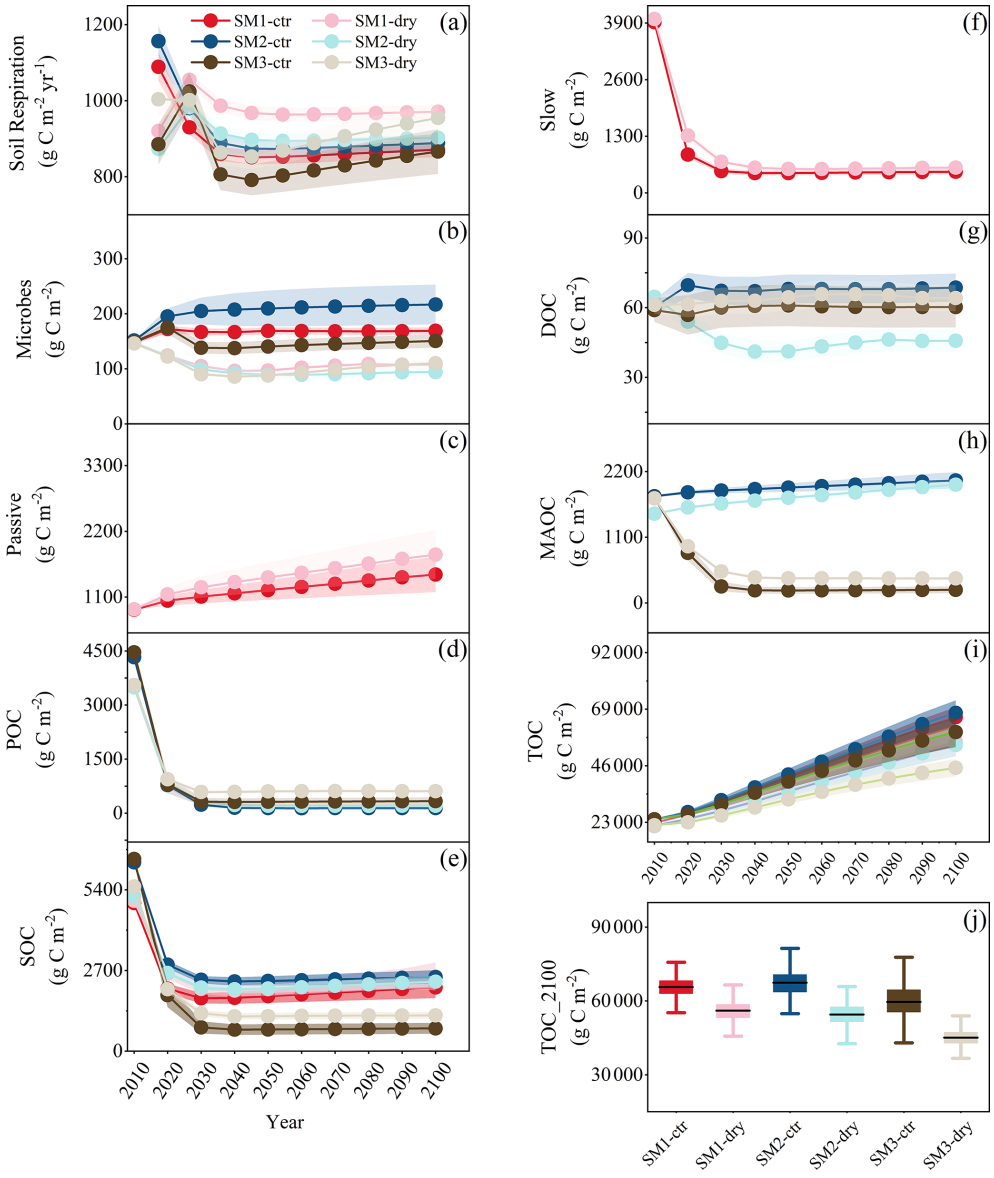

Figure 3. Predicted soil respiration **(a)**, microbial C **(b)**, passive SOM **(c)**, POC **(d)**, SOC **(e)**, slow SOM **(f)**, DOC **(g)**, MAOC **(h)**, total organic C **(i)** from 2014–2100 under dry and control conditions for the three schemes, and **(j)** the mean TOC in 2100 predicted by 1000 simulations.

sponses in turn affect C uptake via photosynthesis and C release via respiration at the ecosystem level, potentially decoupling these two processes (Meir et al., 2008).

Drought consistently reduced microbial biomass carbon (MBC) across all three models, and sensitivity analysis indicated this reduction was primarily driven by increased microbial decay rates (Figs. 2 and A5). With prolonged drought duration, microbial C content exhibited a pattern of initial decline followed by a gradual recovery (Fig. 3b). Drought-induced water stress directly impairs microorganisms, leading to decreased metabolic activity (Quiroga et al., 2024). However, microorganisms can adapt to drought through physiological changes, community turnover, and evolutionary mechanisms (Martiny et al., 2015; Allison, 2023). At the community scale, drought-sensitive microbes may be replaced by more resilient taxa that immigrate into the area (Allison and Martiny, 2008; Ricks and Yannarell, 2023). Several studies have showed that fungi exhibit greater drought adaptability compared to bacteria (Preece et al., 2019; Bastida et al., 2018; Williams and de Vries et al., 2018). Gram-positive bacteria are also better adapted to low-moisture soils compared to Gram-negative bacteria, due to their thicker and harder cell walls, which render them less affected by drought (Castro et al., 2010). Through in situ manipulation experiments at the same site, Bu et al. (2018) and Su et al. (2020b) have observed that drought slightly reduced MBC and mi-

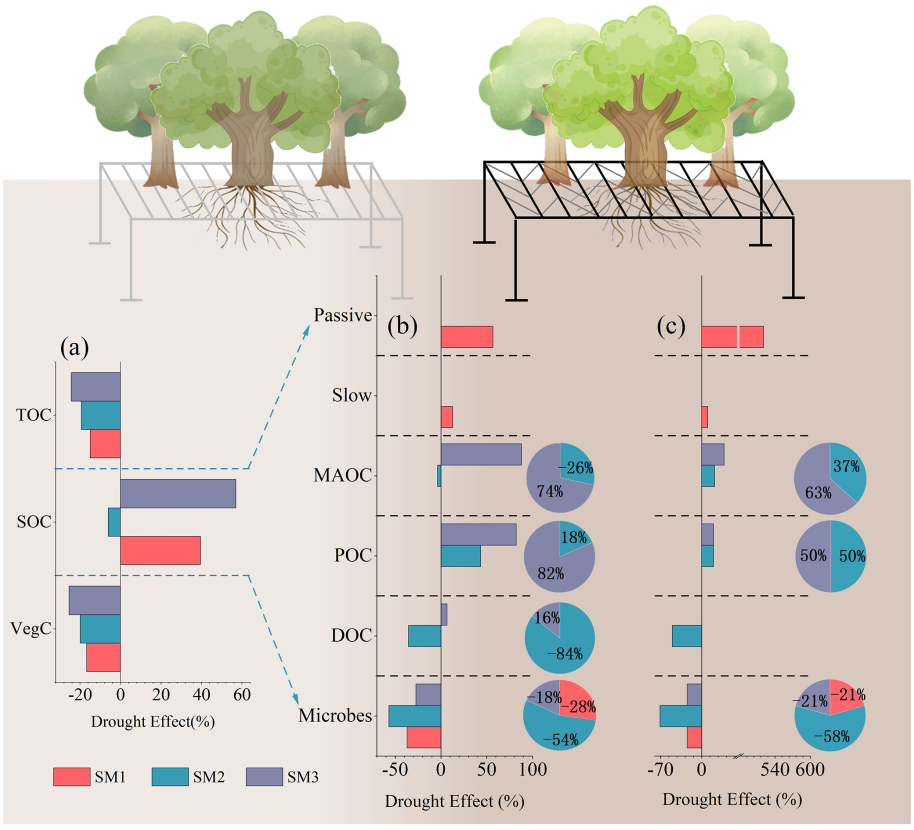

Figure 4. Conceptual diagram illustrating the effects of drought simulated by the three schemes on carbon stocks. **(a)** Drought effects on soil total organic carbon (TOC), soil organic carbon (SOC), and vegetation carbon (VegC) in 2100. **(b)** Drought effects on individual carbon pools; pie charts indicate the proportional contribution of each scheme to the total drought effect on each pool. **(c)** Drought effects on carbon residence time across pools; pie charts represent the proportional contribution of each scheme to the total drought effect on the carbon residence time of each pool.

crobial biomass nitrogen (MBN), and significantly altered the microbial community structure. Drought significantly increased the relative abundance of Acidobacteria, which was primarily associated with the decrease in soil pH, while the relative abundance of Proteobacteria decreased significantly. Besides, the red-yellow soil at the Tiantong site is rich in Fe/Al oxyhydroxides (e.g., hematite, goethite) and kaolinite, which provide a high specific surface area and strong adsorption capacity for microbial necromass and DOC (Wang et al., 2025). Given that microbes directly consume DOC, the incorporation of measured DOC pools in SM2 and SM3 enhances the model's ability to simulate microbial sensitivity to drought (Fig. 4b).

Simulation results from all three modeling schemes consistently showed that drought initially decreased soil respiration, followed by a subsequently recovery (Fig. 3a). This trend mirrors variations in microbial carbon content, indicating that drought regulates soil respiration primarily through its control of microbial biomass (Zhao et al., 2025; Ficken and Warren, 2019). All three schemes consistently simulated an increase in particulate organic carbon (POC) under drought (Fig. 4b). This cross-model consistency arises from multiple ecological mechanisms that are represented, albeit differently, across the three model structures (Du et al., 2015, 2017).

First, drought causes plants to allocate more carbon belowground to acquire water, resulting in the increase in root-to-shoot ratio, root dry weight and root morphological characteristics (Ulrich et al., 2022; Williams and de Vries, 2020; Reinelt et al., 2023). Tracing analysis shows that soil carbon input simulated by the three models increased under drought conditions (Fig. 5d). In situ manipulation experiments found that the specific root length, specific surface area, and fine root biomass of the four dominant local plant species (e.g., *Castanopsis sclerophylla*, *Schima superba*, *Castanopsis carlesii*, *Lithocarpus glaber*) all increased significantly under drought stress (Jiang et al., 2023). This root-derived carbon input is a direct source of POC, as coarse root litter and particulate root fragments are physically classified as POC. In SM1, this increased input enters the slow SOM pool, which functionally overlaps with POC in terms of turnover time and substrate quality (Fig. 5). In SM2 and SM3, these inputs are

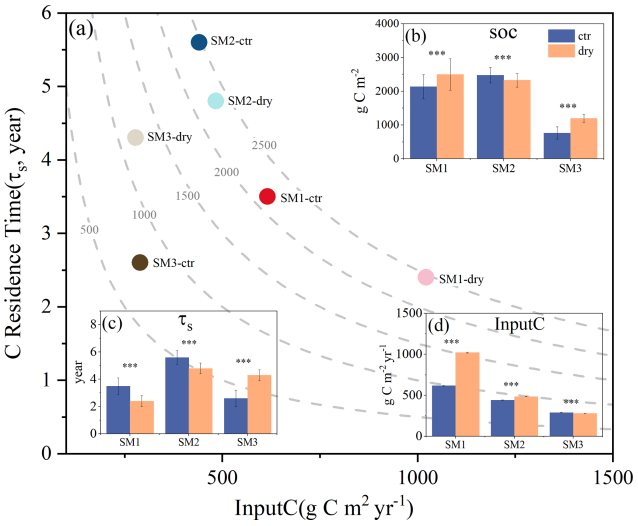

Figure 5. Predicted soil C storage capacity in 2100 by C influx (InputC, x axis) and soil carbon residence time (τ_s, y axis) between control and drought treatments in three model schemes. ***, represents $p < 0.01$.

explicitly routed to the POC pool via litter transfer coefficients (a_{74}, a_{75}).

Second, drought suppresses microbial decomposition activity (Feng et al., 2025). Reduced soil moisture limits extracellular enzyme diffusion, lowers microbial metabolic efficiency, and decreases the activities of POC-degrading enzymes such as cellobiohydrolase and β-glucosidase (Su et al., 2020b; Wu et al., 2025). This suppression is represented in SM1 and SM2 indirectly through soil moisture scalar functions that reduce decomposition rates of all pools, whereas SM3 explicitly captures the reduction via enzyme kinetic parameters (*Vmax*, *KM*) and enzyme-to-microbial carbon ratios (f_{CBH}, f_{BG}, f_{PPO}).

Third, drought-induced changes in soil physicochemical properties suppress the decomposition of SOC. Drought-induced soil aggregate dynamics may physically protect POC from decomposition. Although not explicitly modeled in any of the three schemes, the net effect of reduced POC loss relative to input is emergent in all three model structures. The correlation between soil physicochemical properties and soil carbon mineralization rates indicates that soil moisture content, total carbon (TC), total phosphorus (TP), inorganic nitrogen (IN), available phosphorus (available-P), TC/TP, TN/TP, and IN/available-P are key factors. Soil carbon mineralization rates are positively correlated with soil moisture content, TC/TP, TN/TP, and IN/available-P. Drought led to a decrease in these physicochemical properties. In contrast, soil carbon mineralization rates are negatively correlated with available-P, which increases under drought conditions (Su et al., 2020a).

4.2 Divergent simulations of drought effect on SOC among three modeling schemes

A key divergence among the three modeling schemes lies in their simulation of drought effects on SOC components, which is the key source of discrepancy in the projected carbon storage response (Fig. 4). SM1 divides SOC into three pools, including MBC, slow SOM, and passive SOM. However, since only total SOC data are available to constrain the model, the predictions of this scheme are highly sensitive to the quality and the duration of SOC observations. Given the non-linear response of ecosystems to drought duration (Müller and Bahn, 2022; Anderegg et al., 2020; Schwalm et al., 2017), models constrained by short-term observation data may introduce substantial deviation in long-term projections. In contrast, SM2 partitions the SOC into four observable carbon pools (i.e., Microbes, POC, MAOC and DOC), each independently constrained by corresponding measurements. The trajectory of SOC is thus jointly determined by these four fractions, leading to pronounced differences between the predictions of SM1 and SM2. Given that both models use the same SOC data, this highlights the profound influence of carbon partitioning strategies on model predictions. Furthermore, drought causes the carbon input rates and carbon loss rates of individual carbon pools in SM2 deviate from the overall SOC change rate. These pool-specific discrepancies cause the SOC predictions to diverge increasingly over time between models with different structures.

The differences between SM2 and SM3 are mainly reflected in the dynamics of DOC and MAOC. SM2 employs first-order linear kinetics to describe the decomposition of DOC and MAOC, where the decomposition rate is proportional to their C content. In contrast, SM3 uses reverse Michaelis-Menten kinetics, meaning that SOC decomposition depends not only on substrate carbon content but also on microbial biomass and enzyme activities (Chandel et al., 2023). Under drought, SM2 simulates a decrease in DOC, while SM3 predicts an increase (Fig. 4). Some studies report that drought reduces DOC concentrations (Tiwari et al., 2022; Wu et al., 2023), whereas others suggest it may increase DOC due to factors such as air temperature, soil temperature, humidity, precipitation, pH, and sulfate concentrations (Evans et al., 2005; Sowerby et al., 2010). Sensitivity analysis reveals that DOC in SM2 is influenced mainly by the transfer ratios of POC to DOC and metabolic litter to DOC (Fig. A5). However, in SM3, DOC dynamics are primarily controlled by the microbe maximum assimilation rate and half-saturation for assimilation, indicating that SM3 captures direct microbial regulation of DOC decomposition. Similarly, while SM2 simulates a slight decrease in MAOC under drought, SM3 predicts an increase (Fig. 4). This discrepancy stems the fact that SM3 explicitly incorporates the catalytic effects of three enzyme activities (BG, PPO and CBH) on MAOC decomposition. Long-term drought at this site drives a shift toward fungal-dominated microbial communities (Bu

et al., 2018; Su et al., 2020b). Fungi are major producers of oxidative and hydrolytic enzymes (PPO, CBH, BG). SM3 explicitly represents these enzymes, thereby capturing drought-induced declines in catalytic rates and MAOC accumulation – a key mechanism absent in SM2's implicit microbial representation. This explains why SM3 outperforms SM2 in simulating POC and MAOC dynamics (Fig. A2) and highlights the importance of integrating microbial physiology and site-specific mineralogical and ecological traits into SOC models.

4.3 Implications for future research and model development

Our study enhances the understanding how drought affects forest C dynamic across different model schemes. Nevertheless, we acknowledge that several uncertainties involved in our analysis. First, we only considered three enzymes that directly catalyze soil carbon decomposition. Other enzymes (e.g., Acid phosphatase, N-acetyl-glycosaminidase, Peroxidase) may also contribute indirectly to this process (Su et al., 2020b), but they were not included because their primary roles are in nutrient cycling. Including them would substantially increase model complexity and parameter identifiability issues, especially given the lack of direct constraints from available enzyme activity data. Second, when calculating enzyme activities, we applied laboratory-derived proportional relationships between enzyme quantity and substrate quantity to field conditions, which assumes substrate availability far exceeds enzyme availability in field soils. Finally, laboratory enzyme activity measurements typically use specific substrates, whereas field soils contain multiple potential substrates that could be catalyzed, which introduces additional uncertainty in our simulations.

Although our results demonstrate that incorporating measurable carbon pools or increasing model complexity can improve simulation accuracy for specific carbon fractions and capture nonlinear drought responses, this does not imply that all land surface models should adopt the SM2 or SM3. The appropriate model selection depend on research objectives, data availability, and computational constraints. Specifically, SM1 remains sufficient for large-scale simulations and long-term carbon budget assessments. SM2 is preferable when the goal is to investigate the dynamics of carbon fractions (e.g., POC, MAOC, DOC) and their compositional changes. SM3 becomes essential for exploring nonlinear ecosystem responses to extreme climate events such as drought, warming, or other perturbations. Particularly, the advantages of SM2 and SM3 are contingent upon the availability of observational data for model calibration. Without sufficient constraints, increased complexity can lead to greater parameter uncertainty and reduced robustness. Therefore, future model development should pursue a balanced strategy, introducing additional process representations only when they are supported by data and justified by the specific application.

5 Conclusions

Accurately simulating drought impacts on soil carbon dynamics is critical for predicting terrestrial carbon sequestration. In this study, we integrated data assimilation and traceability analysis to evaluate three soil carbon decomposition schemes, examining how different model structures simulate soil carbon responses to drought. Our results revealed significant disparities in drought effects on soil organic carbon (SOC) among the three models, with these differences primarily driven by variations in carbon input and carbon residence times across pools. Explicitly incorporating microbial enzyme activities notably altered the impacts of drought on mineral-associated organic carbon and dissolved organic carbon. These findings underscore the critical roles of carbon pool partitioning schemes, their empirical constrainability, and the consideration of microbial enzyme catalytic processes in simulating SOC response to drought, thereby advancing our understanding of the complex mechanism governing drought-induced soil organic carbon dynamics.

Appendix A

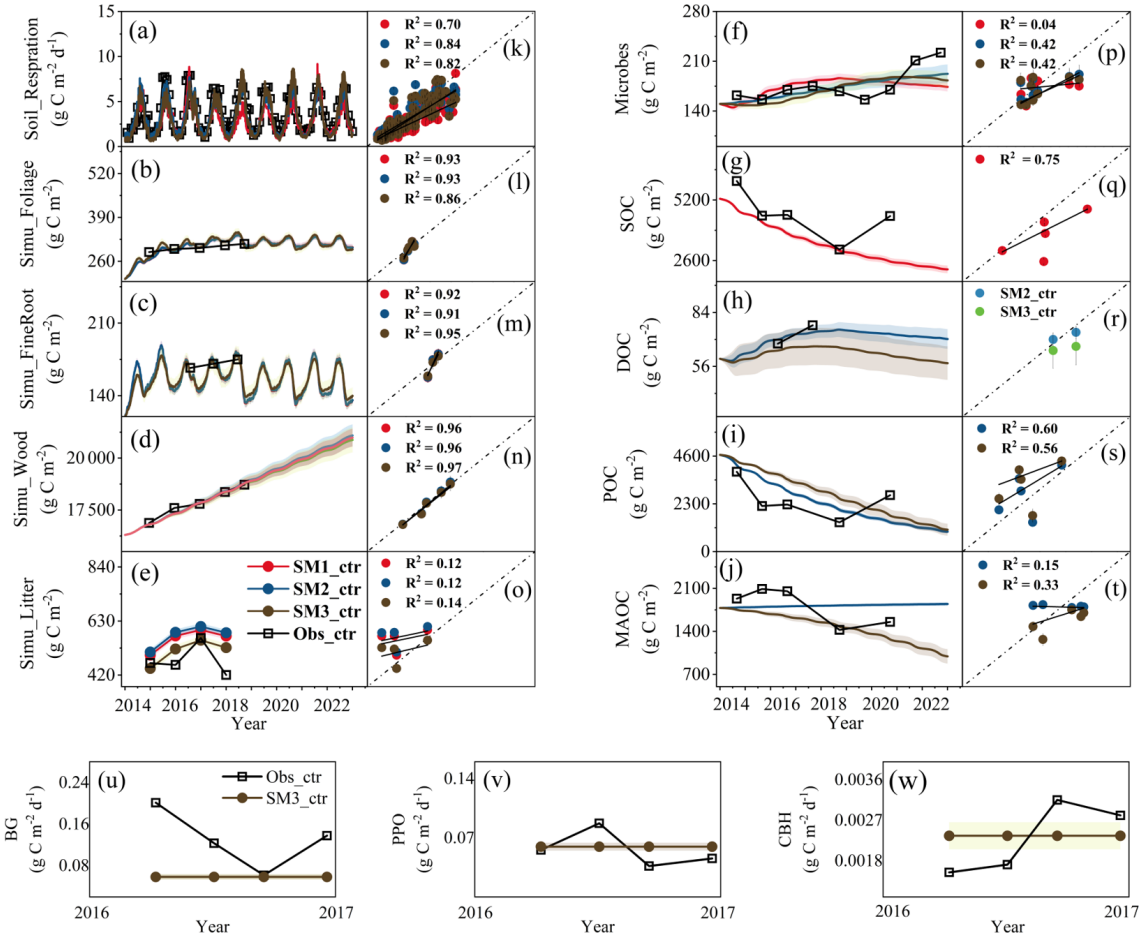

Figure A1. Comparison of the measured values (black squares) and simulated values (lines) in the control conditions of three schemes from 2014 to 2022, $p < 0.05$.

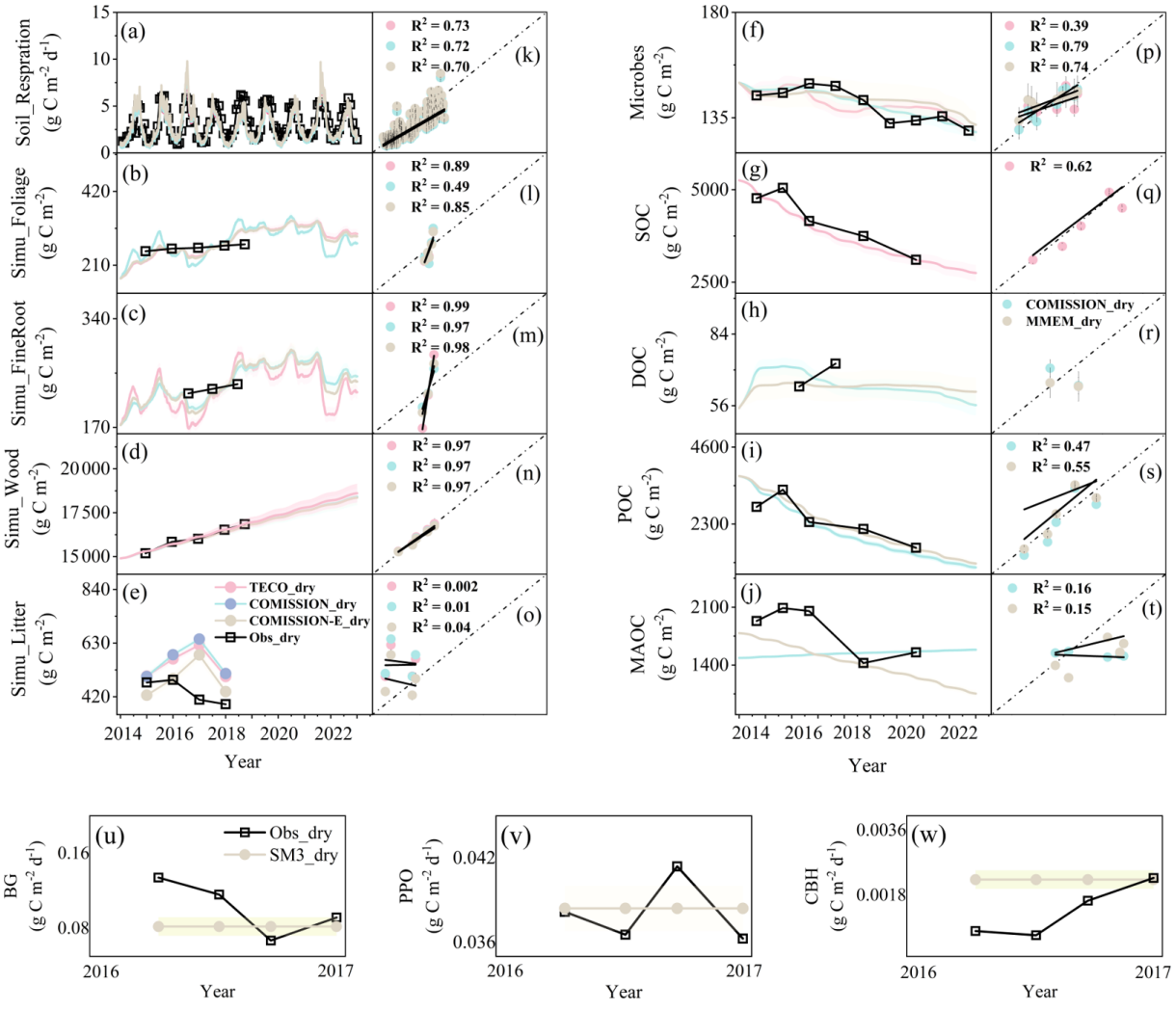

Figure A2. Comparison of the measured values (black squares) and simulated values (lines) in the drought conditions of three schemes from 2014 to 2022, $p < 0.05$.

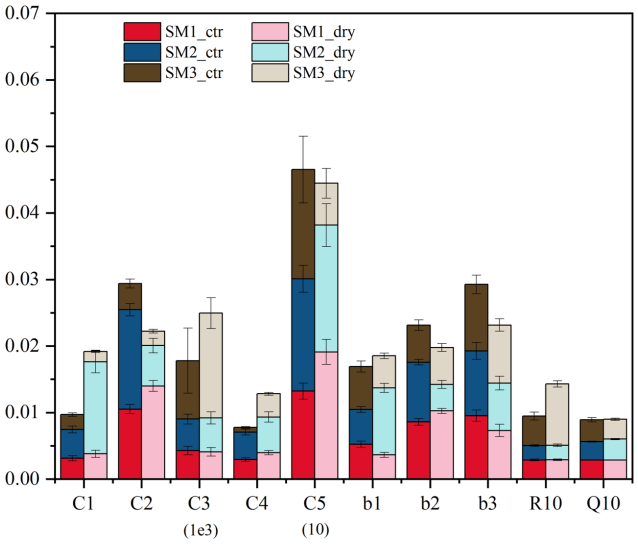

Figure A3. Maximum likelihood value (MLEs) (or means for unconstrained parameters) of the target parameters of vegetations in various models and treatments. Error bars represent standard deviations (SDs). See Table A1 for parameter abbreviations and units.

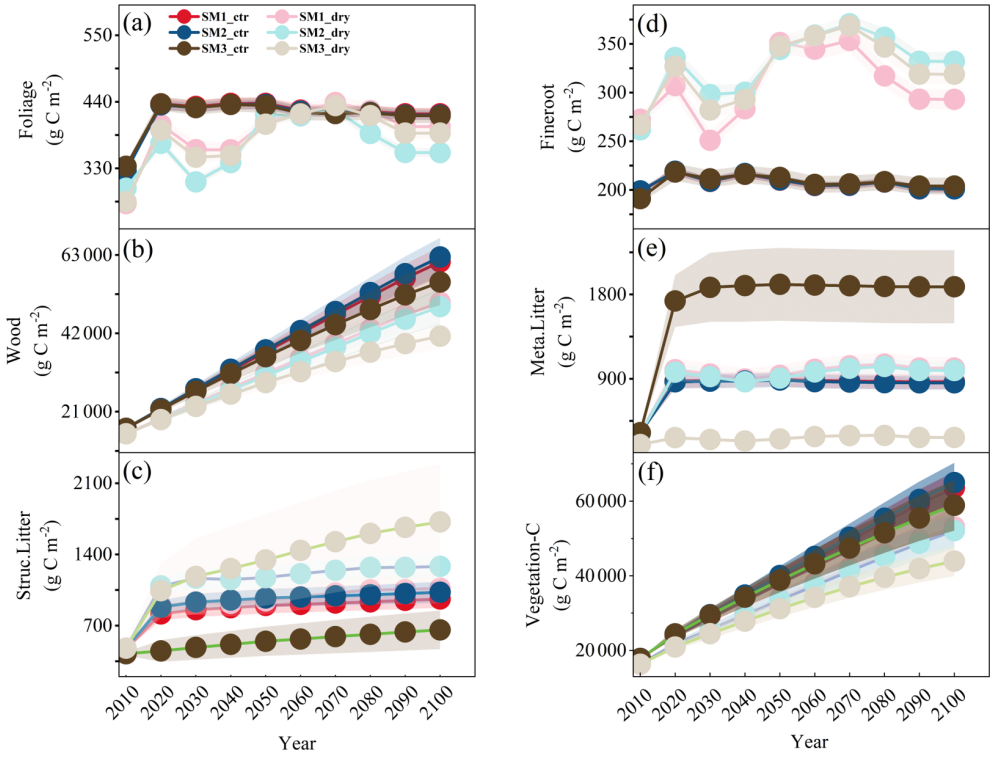

Figure A4. Predicted foliage **(a)**, wood **(b)**, structural litter **(c)**, fineroot **(d)**, Metabolic litter **(e)**, Vegetation C **(f)** from 2014–2100 under dry and control conditions for three schemes.

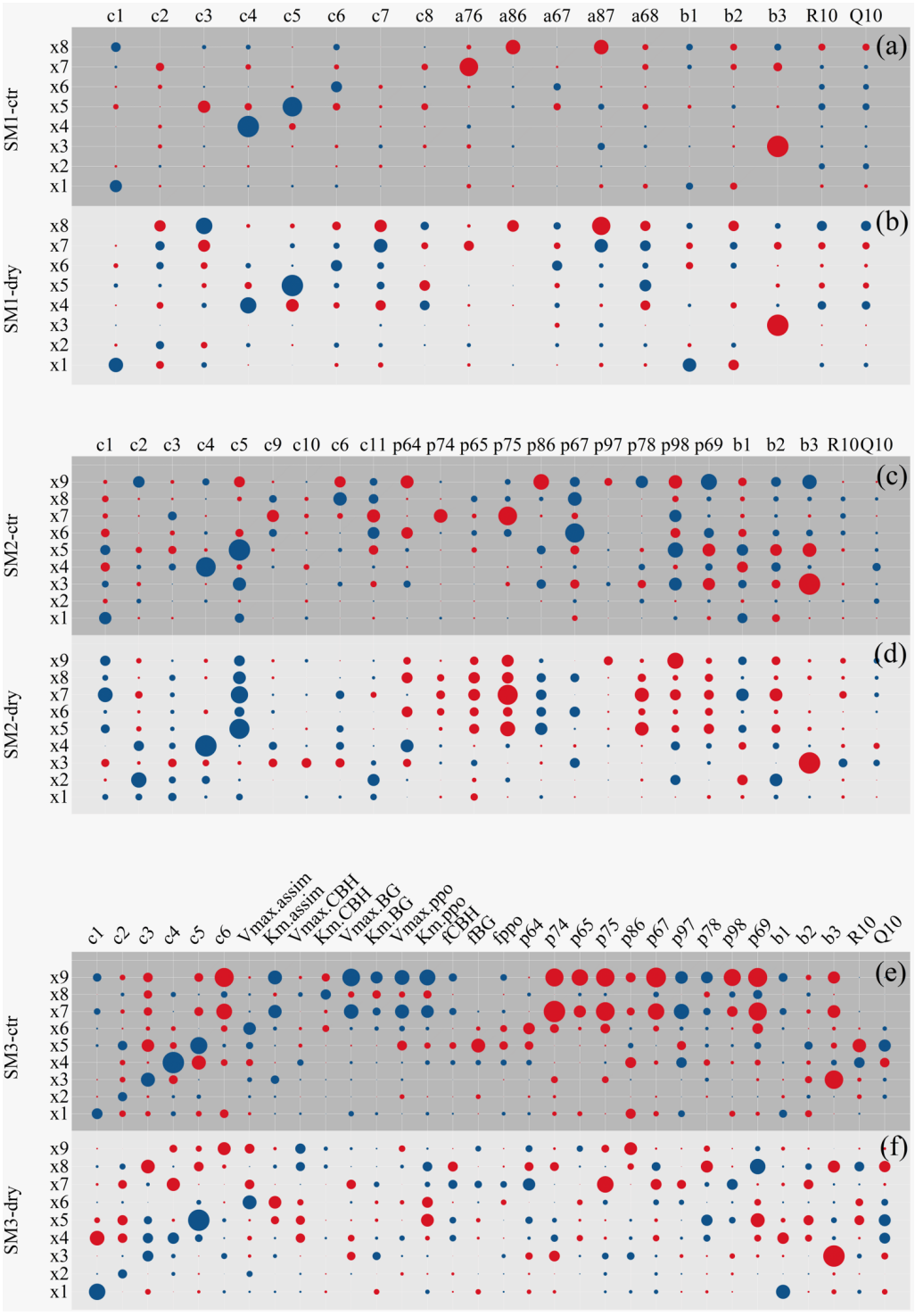

Figure A5. The correlation between carbon pools and model parameters under control and drought conditions of three schemes. Red represents positive correlation and blue represents negative correlation. The *x1, x2, x3, x4, x5* represent the carbon content of foliage, fineroot, wood, metabolic litter, structural litter. *x6, x7, x8* represent microbes slow SOM and passive SOM for SM1. *x6, x7, x8, x9* represent DOC, POC, microbes and MAOC for SM2 and SM3.

Table A1. Target parameters of this study and their prior ranges.

Parameters	Intervals	Unit	Description
C1	0.176–9.95	$mg\,C\,g^{-1}\,d^{-1}$	exit rate of C from foliage
C2	0.176–17.9	$mg\,C\,g^{-1}\,d^{-1}$	exit rate of C from fineroot
C3	0.00176–0.01	$mg\,C\,g^{-1}\,d^{-1}$	exit rate of C from wood
C4	0.274–8.22	$mg\,C\,g^{-1}\,d^{-1}$	exit rate of C from metabolic litter
C5	0.0548–1.64	$mg\,C\,g^{-1}\,d^{-1}$	exit rate of C from structural litter
C6	2.74–13.7	$mg\,C\,g^{-1}\,d^{-1}$	exit rate of C from microbes
C7	0.027–1.37	$mg\,C\,g^{-1}\,d^{-1}$	exit rate of C from slow SOM
C8	0.00137–0.00913	$mg\,C\,g^{-1}\,d^{-1}$	exit rate of C from passive SOM
C9	2.74–68.5	$mg\,C\,g^{-1}\,d^{-1}$	exit rate of C from DOC
C10	0.1–1	$mg\,C\,g^{-1}\,d^{-1}$	exit rate of C from POC
C11	0.00137–0.013	$mg\,C\,g^{-1}\,d^{-1}$	exit rate of C from MAOC
b1	0–0.315	–	allocation of GPP to foliage
b2	0–0.3	–	allocation of GPP to fineroot
b3	0–0.3	–	allocation of GPP to wood
R10	0–1	$g\,C\,m^{-2}\,d^{-1}$	basic respiration rate
Q10	2–5	–	temperature sensitivity of respiration
a76	0–0.5	–	allocation of microbes to slow SOM
a86	0–0.5	–	allocation of microbes to passive SOM
a67	0–0.5	–	allocation of slow SOM to microbes
a87	0–0.5	–	allocation of slow SOM to passive SOM
a68	0–1	–	allocation of passive SOM to microbes
p64	0–0.3	–	allocation of metabolic litter to DOC
p74	0–0.7	–	allocation of metabolic litter to POC
p65	0–0.6	–	allocation of structural litter to DOC
p75	0–0.4	–	allocation of structural litter to POC
p86	0–0.7	–	allocation of DOC to microbes
p67	0–0.8	–	allocation of POC to DOC
p97	0–0.2	–	allocation of POC to MAOC
p78	0–0.7	–	allocation of microbes to POC
p98	0–0.3	–	allocation of microbes to MAOC
p69	0–0.8	–	allocation of MAOC to DOC
$V_{max.assim}$	0.001–0.4	$mg\,C\,mg^{-1}\,MBC\,d^{-1}$	microbe maximum assimilation rate
$Km_{.assim}$	300–3000	$g\,C\,m^{-3}$	half-saturation for assimilation
$V_{max.CBH}$	0.0001–0.01	$mg\,C\,mg^{-1}\,CBH\,d^{-1}$	maximum reaction rate of CBH
$Km_{.CBH}$	300–3000	$g\,C\,m^{-3}$	half-saturation for reaction of CBH
$V_{max.PPO}$	0.0001–0.2	$mg\,C\,mg^{-1}\,PPO\,d^{-1}$	maximum reaction rate of PPO
$Km_{.PPO}$	300–6000	$g\,C\,m^{-3}$	half-saturation for reaction of PPO
$V_{max.BG}$	0.0001–0.2	$mg\,C\,mg^{-1}\,BG\,d^{-1}$	maximum reaction rate of BG
$Km_{.BG}$	300–3000	$g\,C\,m^{-3}$	half-saturation for reaction of BG
f_{CBH}	0–0.01	–	CBH-to-microbial carbon ratio
f_{PPO}	0–0.2	–	PPO-to-microbial carbon ratio
f_{BG}	0–0.1	–	BG-to-microbial carbon ratio

Data availability. Data will be made available on request.

Author contributions. FD and ZD collected and analyzed the data and wrote the manuscript. ZD conceived, designed, and oversaw the study. FD, LF, and ZG conducted the statistical analysis. FD, XZ, and ZD discussed, wrote, and revised the manuscript with major contributions from LZ. YZ and GZ commented on the manuscript.

Competing interests. The contact author has declared that none of the authors has any competing interests.

Disclaimer. Publisher's note: Copernicus Publications remains neutral with regard to jurisdictional claims made in the text, published maps, institutional affiliations, or any other geographical representation in this paper. The authors bear the ultimate responsibility for providing appropriate place names. Views expressed in the text are those of the authors and do not necessarily reflect the views of the publisher.

Financial support. This research was financially supported by the National Natural Science Foundation of China (Grant no. 32241032, 31930072, 32471683, 32071593) and the Fundamental Research Funds for the Central Universities (Grant no. 2572022BA08); Heilongjiang Touyan Innovation Team Program (Forest Carbon Sink Assessment and Carbon Sequestration Management Innovation Team).

Review statement. This paper was edited by Anja Rammig and reviewed by two anonymous referees.

References

Abramoff, R. Z., Guenet, B., Zhang, H. C., Georgiou, K., Xu, X. F., Rossel, R. A. V., Yuan, W. P., and Ciais, P.: Improved global-scale predictions of soil carbon stocks with Millennial Version 2, Soil Biol. Biochem., 164, https://doi.org/10.1016/j.soilbio.2021.108466, 2022.

Allison, S. D.: Microbial drought resistance may destabilize soil carbon, Trends Microbiol., 31, 780–787, https://doi.org/10.1016/j.tim.2023.03.002, 2023.

Allison, S. D. and Martiny, J. B. H.: Resistance, resilience, and redundancy in microbial communities, P. Natl. Acad. Sci. USA, 105, 11512–11519, https://doi.org/10.1073/pnas.0801925105, 2008.

Allison, S. D., Wallenstein, M. D., and Bradford, M. A.: Soil-carbon response to warming dependent on microbial physiology, Nat. Geosci., 3, 336–340, https://doi.org/10.1038/NGEO846, 2010.

Anderegg, W. R. L., Trugman, A. T., Badgley, G., Konings, A. G., and Shaw, J.: Divergent forests sensitivity to repeated extreme droughts, Nat. Clim. Change, 10, 1091-U19, https://doi.org/10.1038/s41558-020-00919-1, 2020.

Barnard, R. L., Osborne, C. A., and Firestone, M. K.: Responses of soil bacterial and fungal communities to extreme desiccation and rewetting, ISME J., 7, 2229–2241, https://doi.org/10.1038/ismej.2013.104, 2013.

Basile-Doelsch, I., Balesdent, J., and Pellerin, S.: Reviews and syntheses: The mechanisms underlying carbon storage in soil, Biogeosciences, 17, 5223–5242, https://doi.org/10.5194/bg-17-5223-2020, 2020.

Bastida, F., Torres, I. F., Andrés-Abellán, M., Baldrian, P., López-Mondéjar, R., Vetrovsky, T., and Jehmlich, N.: Differential sensitivity of total and active soil microbial communities to drought and forest management, Glob. Change Biol., 24, 552–552, https://doi.org/10.1111/gcb.13953, 2018.

Benbi, D. K., Boparai, A. K., and Brar, K.: Decomposition of particulate organic matter is more sensitive to temperature than the mineral associated organic matter, Soil Biol. Biochem., 70, 183–192, https://doi.org/10.1016/j.soilbio.2013.12.032, 2014.

Blankinship, J. C., Fonte, S. J., Six, J., and Schimel, J. P.: Plant versus microbial controls on soil aggregate stability in a seasonally dry ecosystem, Geoderma, 272, https://doi.org/10.1016/j.geoderma.2016.03.008, 2016.

Bu, X. L., Gu, X. Y., Zhou, X. Q., Zhang, M. Y., Zhang, M. Y., Zhang, J., Zhou, X. H., Chen, X. Y., and Wang, X. H.: Extreme drought slightly decreased soil labile organic C and N contents and altered microbial community structure in a subtropical evergreen forest, Forest Ecol. Manag., 429, 18–27, https://doi.org/10.1016/j.foreco.2018.06.036, 2018.

Caldwell, B. A.: Enzyme activities as a component of soil biodiversity: A review, Pedobiologia, 49, 637–644, https://doi.org/10.1016/j.pedobi.2005.06.003, 2005.

Camino-Serrano, M., Guenet, B., Luyssaert, S., Ciais, P., Bastrikov, V., De Vos, B., Gielen, B., Gleixner, G., Jornet-Puig, A., Kaiser, K., Kothawala, D., Lauerwald, R., Peñuelas, J., Schrumpf, M., Vicca, S., Vuichard, N., Walmsley, D., and Janssens, I. A.: ORCHIDEE-SOM: modeling soil organic carbon (SOC) and dissolved organic carbon (DOC) dynamics along vertical soil profiles in Europe, Geosci. Model Dev., 11, 937–957, https://doi.org/10.5194/gmd-11-937-2018, 2018.

Campbell, C. A.: Soil organic carbon, nitrogen, and fertility, Dev. Soil Sci., 8, 173–271, https://doi.org/10.1016/S0166-2481(08)70020-5, 1978.

Castro, H. F., Classen, A. T., Austin, E. E., Norby, R. J., and Schadt, C. W.: Soil Microbial Community Responses to Multiple Experimental Climate Change Drivers, Appl. Environ. Microb., 76, 999–1007, https://doi.org/10.1128/AEM.02874-09, 2010.

Chandel, A. K., Jiang, L. F., and Luo, L. Q.: Microbial Models for Simulating Soil Carbon Dynamics: A Review, J. Geophys. Res.-Biogeo., 128, https://doi.org/10.1029/2023JG007436, 2023.

Chen, J., Luo, Y. Q., van Groenigen, K. J., Hungate, B. A., Cao, J. J., Zhou, X. H., and Wang, R. W.: A keystone microbial enzyme for nitrogen control of soil carbon storage, Sci. Adv., 4, https://doi.org/10.1126/sciadv.aaq1689, 2018.

Choat, B., Brodribb, T. J., Brodersen, C. R., Duursma, R. A., López, R., and Medlyn, B. E.: Triggers of tree mortality under drought, Nature, 558, 531–539, https://doi.org/10.1038/s41586-018-0240-x, 2018.

Citerne, N., Wallace, H. M., Lewis, T., Reverchon, F., Omidvar, N., Hu, H. W., Shi, X. Z., Zhou, X. H., Zhou, G. Y., Farrar, M., Rashti, M. R., and Bai, S. H.: Effects of Biochar on Pulse C and N

Cycling After a Short-term Drought: a Laboratory Study, J. Soil Sci. Plant Nut., 21, 2815–2825, https://doi.org/10.1007/s42729-021-00568-z, 2021.

Cotrufo, M. F. and Lavallee, J. M.: Soil organic matter formation, persistence, and functioning: A synthesis of current understanding to inform its conservation and regeneration, Adv. Agron., 172, 1–66, https://doi.org/10.1016/bs.agron.2021.11.002, 2022.

Cotrufo, M. F., Wallenstein, M. D., Boot, C. M., Denef, K., and Paul, E.: The Microbial Efficiency-Matrix Stabilization (MEMS) framework integrates plant litter decomposition with soil organic matter stabilization: do labile plant inputs form stable soil organic matter?, Glob. Change Biol., 19, 988–995, https://doi.org/10.1111/gcb.12113, 2013.

Cotrufo, M. F., Ranalli, M. G., Haddix, M. L., Six, J., and Lugato, E.: Soil carbon storage informed by particulate and mineral-associated organic matter, Nat. Geosci., 12, 989–994, https://doi.org/10.1038/s41561-019-0484-6, 2019.

de Vries, F. T., Griffiths, R. I., Bailey, M., Craig, H., Girlanda, M., Gweon, H. S., Hallin, S., Kaisermann, A., Keith, A. M., Kretzschmar, M., Lemanceau, P., Lumini, E., Mason, K. E., Oliver, A., Ostle, N., Prosser, J. I., Thion, C., Thomson, B., and Bardgett, R. D.: Soil bacterial networks are less stable under drought than fungal networks, Nat. Commun., 9, https://doi.org/10.1038/s41467-018-05516-7, 2018.

Du, F. F., Zhang, Y. M., Zhou, L. Y., Dietrich, P., Zhou, G. Y., Wang, J., Zhang, Q. Z., Wang, X. C., Du, Z. G., and Zhou, X. H.: Similar carbon accumulation rates with distinct drivers in two temperate forest restoration approaches, Catena, 258, https://doi.org/10.1016/j.catena.2025.109249, 2025.

Du, Z. G., Nie, Y. Y., He, Y. H., Yu, G. R., Wang, H. M., and Zhou, X. H.: Complementarity of flux- and biometric-based data to constrain parameters in a terrestrial carbon model, Tellus B, 67, https://doi.org/10.3402/tellusb.v67.24102, 2015.

Du, Z. G., Zhou, X. H., Shao, J. J., Yu, G. R., Wang, H. M., Zhai, D. P., Xia, J. Y., and Luo, Y. Q.: Quantifying uncertainties from additional nitrogen data and processes in a terrestrial ecosystem model with Bayesian probabilistic inversion, J. Adv. Model. Earth Sy., 9, 548–565, https://doi.org/10.1002/2016MS000687, 2017.

Eastman, B. A., Wieder, W. R., Hartman, M. D., Brzostek, E. R., and Peterjohn, W. T.: Can models adequately reflect how long-term nitrogen enrichment alters the forest soil carbon cycle?, Biogeosciences, 21, 201–221, https://doi.org/10.5194/bg-21-201-2024, 2024.

Evans, C. D., Monteith, D. T., and Cooper, D. M.: Long-term increases in surface water dissolved organic carbon: Observations, possible causes and environmental impacts, Environ. Pollut., 137, 55–71, https://doi.org/10.1016/j.envpol.2004.12.031, 2005.

Feng, J., Yao, Y., He, Y., Wang, P., Hu, H., and Zhang, S.: Hydraulic strategies of Cunninghamia lanceolata under drought are shaped by native drought conditions, For. Res., 5, e031, https://doi.org/10.48130/forres-0025-0031, 2025.

Ficken, C. D. and Warren, J. M.: The carbon economy of drought: comparing respiration responses of roots, mycorrhizal fungi, and free-living microbes to an extreme dry-rewet cycle, Plant Soil, 435, 407–422, https://doi.org/10.1007/s11104-018-03900-2, 2019.

Gao, Q., Hasselquist, N. J., Palmroth, S., Zheng, Z. M., and You, W. H.: Short-term response of soil respiration to nitrogen fertilization in a subtropical evergreen forest, Soil Biol. Biochem., 76, 297–300, https://doi.org/10.1016/j.soilbio.2014.04.020, 2014.

Guo, X. W., Rossel, R. A. V., Wang, G. C., Xiao, L. J., Wang, M. M., Zhang, S., and Luo, Z. K.: Particulate and mineral-associated organic carbon turnover revealed by modelling their long-term dynamics, Soil Biol. Biochem., 173, https://doi.org/10.1016/j.soilbio.2022.108780, 2022.

Han, Y. A., Deng, J. J., Zhou, W. M., Wang, Q. M., and Yu, D. P.: Seasonal Responses of Hydraulic Function and Carbon Dynamics in Spruce Seedlings to Continuous Drought, Front. Plant Sci., 13, https://doi.org/10.3389/fpls.2022.868108, 2022.

Hansen, P. M., Even, R., King, A. E., Lavallee, J., Schipanski, M., and Cotrufo, M. F.: Distinct, direct and climate-mediated environmental controls on global particulate and mineral-associated organic carbon storage, Glob. Change Biol., 30, https://doi.org/10.1111/gcb.17080, 2024.

Hao, X. C. and Singh, V. P.: Drought characterization from a multivariate perspective: A review, J. Hydrol., 527, 668–678, https://doi.org/10.1016/j.jhydrol.2015.05.031, 2015.

Honeker, L. K., Pugliese, G., Ingrisch, J., Fudyma, J., Gil-Loaiza, J., Carpenter, E., Singer, E., Hildebrand, G., Shi, L. L., Hoyt, D. W., Chu, R. K., Toyoda, J., Krechmer, J. E., Claflin, M. S., Ayala-Ortiz, C., Freire-Zapata, V., Pfannerstill, E. Y., Daber, L. E., Meeran, K., Dippold, M. A., Kreuzwieser, J., Williams, J., Ladd, S. N., Werner, C., Tfaily, M. M., and Meredith, L. K.: Drought re-routes soil microbial carbon metabolism towards emission of volatile metabolites in an artificial tropical rainforest, Nat. Microbiol., 9, 1146–1147, https://doi.org/10.1038/s41564-023-01507-7, 2024.

Huang, Y., Guenet, B., Ciais, P., Janssens, I. A., Soong, J. L., Wang, Y., Goll, D., Blagodatskaya, E., and Huang, Y.: ORCHIMIC (v1.0), a microbe-mediated model for soil organic matter decomposition, Geosci. Model Dev., 11, 2111–2138, https://doi.org/10.5194/gmd-11-2111-2018, 2018.

Hueso, S., García, C., and Hernández, T.: Severe drought conditions modify the microbial community structure, size and activity in amended and unamended soils, Soil Biol. Biochem., 50, 167–173, https://doi.org/10.1016/j.soilbio.2012.03.026, 2012.

IPCC: Climate Change 2023: Synthesis Report. Contribution of Working Groups I, II and III to the Sixth Assessment Report of the Intergovernmental Panel on Climate Change, edited by: Core Writing Team, Lee, H., and Romero, J., IPCC, Geneva, Switzerland, 35–115, https://doi.org/10.59327/IPCC/AR6-9789291691647, 2023.

Jenny, H.: Factors of Soil Formation: A System of Quantitative Pedology, Dover Publications, New York, 281 pp., ISBN 978-0486642880, 1941.

Jiang, Z., Fu, Y., Zhou, L., He, Y., Zhou, G., Dietrich, P., Long, J., Wang, X., Jia, S., Ji, Y., Jia, Z., Song, B., Liu, R., and Zhou, X.: Plant growth strategy determines the magnitude and direction of drought-induced changes in root exudates in subtropical forests, Glob. Change Biol., 29, 3476–3488, 2023.

Knorr, W., Prentice, I. C., House, J. I., and Holland, E. A.: Long-term sensitivity of soil carbon turnover to warming, Nature, 433, 298–301, https://doi.org/10.1038/nature03226, 2005.

Krinner, G., Viovy, N., de Noblet-Ducoudré, N., Ogée, J., Polcher, J., Friedlingstein, P., Ciais, P., Sitch, S., and Prentice, I. C.: A dynamic global vegetation model for studies of the cou-

pled atmosphere-biosphere system, Global Biogeochem. Cy., 19, GB1015, https://doi.org/10.1029/2003GB002199, 2005.

Lawrence, C. R., Neff, J. C., and Schimel, J. P.: Does adding microbial mechanisms of decomposition improve soil organic matter models? A comparison of four models using data from a pulsed rewetting experiment, Soil Biol. Biochem., 41, 1923–1934, https://doi.org/10.1016/j.soilbio.2009.06.016, 2009.

Lawrence, D. M., Fisher, R. A., Koven, C. D., Oleson, K. W., Swenson, S. C., Bonan, G., Collier, N., Ghimire, B., van Kampenhout, L., Kennedy, D., Kluzek, E., Lawrence, P. J., Li, F., Li, H. Y., Lombardozzi, D., Riley, W. J., Sacks, W. J., Shi, M. J., Vertenstein, M., Wieder, W. R., Xu, C. G., Ali, A. A., Badger, A. M., Bisht, G., van den Broeke, M., Brunke, M. A., Burns, S. P., Buzan, J., Clark, M., Craig, A., Dahlin, K., Drewniak, B., Fisher, J. B., Flanner, M., Fox, A. M., Gentine, P., Hoffman, F., Keppel-Aleks, G., Knox, R., Kumar, S., Lenaerts, J., Leung, L. R., Lipscomb, W. H., Lu, Y. Q., Pandey, A., Pelletier, J. D., Perket, J., Randerson, J. T., Ricciuto, D. M., Sanderson, B. M., Slater, A., Subin, Z. M., Tang, J. Y., Thomas, R. Q., Martin, M. V., and Zeng, X. B.: The Community Land Model Version 5: Description of New Features, Benchmarking, and Impact of Forcing Uncertainty, J. Adv. Model. Earth Sy., 11, 4245–4287, https://doi.org/10.1029/2018MS001583, 2019.

Lee, J. and Rossel, R. V. A.: Soil carbon simulation confounded by different pool initialization, Nutr. Cycl. Agroecosys., 116, 245–255, https://doi.org/10.1007/s10705-019-10041-0, 2020.

Liang, C., Kästner, M., and Joergensen, R. G.: Microbial necromass on the rise: The growing focus on its role in soil organic matter development, Soil Biol. Biochem, 150, https://doi.org/10.1016/j.soilbio.2020.108000, 2020.

Lugato, E., Lavallee, J. M., Haddix, M. L., Panagos, P., and Cotrufo, M. F.: Different climate sensitivity of particulate and mineral-associated soil organic matter, Nat. Geosci., 15, 509–509, https://doi.org/10.1038/s41561-022-00945-y, 2022.

Luo, Z. K., Luo, Y. Q., Wang, G. C., Xia, J. Y., and Peng, C. H.: Warming-induced global soil carbon loss attenuated by downward carbon movement, Glob. Change Biol., 26, 7242–7254, https://doi.org/10.1111/gcb.15370, 2020.

Martiny, J. B. H., Jones, S. E., Lennon, J. T., and Martiny, A. C.: Microbiomes in light of traits: A phylogenetic perspective, Science, 350, https://doi.org/10.1126/science.aac9323, 2015.

Meir, P., Metcalfe, D. B., Costa, A. C. L., and Fisher, R. A.: The fate of assimilated carbon during drought: impacts on respiration in Amazon rainforests, Philos. T. R. Soc. B, 363, 1849–1855, https://doi.org/10.1098/rstb.2007.0021, 2008.

Moorhead, D. L. and Sinsabaugh, R. L.: A theoretical model of litter decay and microbial interaction, Ecol. Monogr., 76, 151–174, https://doi.org/10.1890/0012-9615(2006)076[0151:ATMOLD]2.0.CO;2, 2006.

Müller, L. M. and Bahn, M.: Drought legacies and ecosystem responses to subsequent drought, Glob. Change Biol., 28, 5086–5103, https://doi.org/10.1111/gcb.16270, 2022.

Paul, E. A. and Van Vee, J. A.: The use of tracers to determine the dynamic nature of organic matter, Trans. Int. Congr. Soil Sci., 11, 61–102, 1978.

Pennisi, E.: Global drought experiment reveals the toll on plant growth, Science, 377, 901–910, https://doi.org/10.1126/science.ade5540, 2022.

Preece, C., Verbruggen, E., Liu, L., Weedon, J. T., and Peñuelas, J.: Effects of past and current drought on the composition and diversity of soil microbial communities, Soil Biol. Biochem., 131, 28–39, https://doi.org/10.1016/j.soilbio.2018.12.022, 2019.

Quiroga, G., Castagneyrol, B., Abdala-Roberts, L., and Moreira, X.: A meta-analysis of the effects of climate change-related abiotic factors on aboveground and belowground plant-associated microbes, Oikos, 2024, https://doi.org/10.1111/oik.10411, 2024.

Reinelt, L., Whitaker, J., Kazakou, E., Bonnal, L., Bastianelli, D., Bullock, J. M., and Ostle, N. J.: Drought effects on root and shoot traits and their decomposability, Funct. Ecol., 37, 1044–1054, https://doi.org/10.1111/1365-2435.14261, 2023.

Ricks, K. D. and Yannarell, A. C.: Soil moisture incidentally selects for microbes that facilitate locally adaptive plant response, P. Roy. Soc. B-Biol. Sci., 290, https://doi.org/10.1098/rspb.2023.0469, 2023.

Rowland, L., Ramírez-Valiente, J. A., Hartley, I. P., and Mencuccini, M.: How woody plants adjust above- and below-ground traits in response to sustained drought, New Phytol., 239, 1173–1189, https://doi.org/10.1111/nph.19000, 2023.

Saiya-Cork, K. R., Sinsabaugh, R. L., and Zak, D. R.: The effects of long term nitrogen deposition on extracellular enzyme activity in an Acer Saccharum forest soil, Soil Biol. Biochem., 34, 1309–1315, https://doi.org/10.1016/S0038-0717(02)00074-3, 2002.

Sardans, J. and Peñuelas, J.: Soil Enzyme Activity in a Mediterranean Forest after Six Years of Drought, Soil Sci. Soc. Am. J., 74, 838–851, https://doi.org/10.2136/sssaj2009.0225, 2010.

Schimel, J. P.: Life in Dry Soils: Effects of Drought on Soil Microbial Communities and Processes, Annu. Rev. Ecol. Evol. S., 49, 409–432, https://doi.org/10.1146/annurev-ecolsys-110617-062614, 2018.

Schwalm, C. R., Anderegg, W. R. L., Michalak, A. M., Fisher, J. B., Biondi, F., Koch, G., Litvak, M., Ogle, K., Shaw, J. D., Wolf, A., Huntzinger, D. N., Schaefer, K., Cook, R., Wei, Y. X., Fang, Y. Y., Hayes, D., Huang, M. Y., Jain, A., and Tian, H. Q.: Global patterns of drought recovery, Nature, 548, 202–205, https://doi.org/10.1038/nature23021, 2017.

Si, Q., Chen, K., Wei, B., Zhang, Y., Sun, X., and Liang, J.: Dissolved carbon flow to particulate organic carbon enhances soil carbon sequestration, SOIL, 10, 441–450, https://doi.org/10.5194/soil-10-441-2024, 2024.

Sokol, N. W., Sanderman, J., and Bradford, M. A.: Pathways of mineral-associated soil organic matter formation: Integrating the role of plant carbon source, chemistry, and point of entry, Glob. Change Biol., 25, 12–24, https://doi.org/10.1111/gcb.14482, 2019.

Sowerby, A., Emmett, B. A., Williams, D., Beier, C., and Evans, C. D.: The response of dissolved organic carbon (DOC) and the ecosystem carbon balance to experimental drought in a temperate shrubland, Eur. J. Soil Sci., 61, 697–709, https://doi.org/10.1111/j.1365-2389.2010.01276.x, 2010.

Stursová, M., Zifcáková, L., Leigh, M. B., Burgess, R., and Baldrian, P.: Cellulose utilization in forest litter and soil: identification of bacterial and fungal decomposers, FEMS Microbiol. Ecol., 80, 735–746, https://doi.org/10.1111/j.1574-6941.2012.01343.x, 2012.

Su, X., Su, X. L., Yang, S. C., Zhou, G. Y., Ni, M. Y., Wang, C., Qin, H., Zhou, X. H., and Deng, J.: Drought changed soil organic carbon composition and bacterial carbon metabolizing pat-

terns in a subtropical evergreen forest, Sci. Total Environ., 736, https://doi.org/10.1016/j.scitotenv.2020.139568, 2020a.

Su, X. L., Su, X., Zhou, G. Y., Du, Z. G., Yang, S. C., Ni, M. Y., Qin, H., Huang, Z. Q., Zhou, X. H., and Deng, J.: Drought accelerated recalcitrant carbon loss by changing soil aggregation and microbial communities in a subtropical forest, Soil Biol. Biochem., 148, https://doi.org/10.1016/j.soilbio.2020.107898, 2020b.

Szejgis, J., Carrillo, Y., Jeffries, T. C., Dijkstra, F. A., Chieppa, J., Horn, S., Bristol, D., Maisnam, P., Eldridge, D., and Nielsen, U. N.: Altered rainfall greatly affects enzyme activity but has limited effect on microbial biomass in Australian dryland soils, Soil Biol. Biochem., 189, https://doi.org/10.1016/j.soilbio.2023.109277, 2024.

Tao, F., Houlton, B. Z., Huang, Y. Y., Wang, Y. P., Manzoni, S., Ahrens, B., Mishra, U., Jiang, L. F., Huang, X. M., and Luo, Y. Q.: Convergence in simulating global soil organic carbon by structurally different models after data assimilation, Glob. Change Biol., 30, https://doi.org/10.1111/gcb.17297, 2024.

Tiwari, T., Sponseller, R., and Laudon, H.: The emerging role of drought as a regulator of dissolved organic carbon in boreal landscapes, Nat. Commun., 13, https://doi.org/10.1038/s41467-022-32839-3, 2022.

Ulrich, D. E. M., Clendinen, C. S., Alongi, F., Mueller, R. C., Chu, R. K., Toyoda, J., Gallegos-Graves, L., Goemann, H. M., Peyton, B., Sevanto, S., and Dunbar, J.: Root exudate composition reflects drought severity gradient in blue grama (Bouteloua gracilis), Sci. Rep.-UK, 12, https://doi.org/10.1038/s41598-022-16408-8, 2022.

Villarino, S. H., Pinto, P., Jackson, R. B., and Piñeiro, G.: Plant rhizodeposition: A key factor for soil organic matter formation in stable fractions, Sci Adv., 7, https://doi.org/10.1126/sciadv.abd3176, 2021.

Wan, F., Bian, C., Weng, E., Luo, Y., Huang, K., and Xia, J.: TECO-CNP Sv1.0: a coupled carbon-nitrogen-phosphorus model with data assimilation for subtropical forests, Geosci. Model Dev., 18, 7545–7573, https://doi.org/10.5194/gmd-18-7545-2025, 2025.

Wang, X., Zhou, L., Fu, Y., Jiang, Z., Jia, S., Song, B., Liu, D., and Zhou, X.: Drought-induced changes in rare microbial community promoted contribution of microbial necromass C to SOC in a subtropical forest, Soil Biol. Biochem., 189, https://doi.org/10.1016/j.soilbio.2023.109252, 2024.

Wang, X. Y., Lu, D. L., Schonbeck, L., Han, Y. N., Bai, S. B., Yu, D. P., Han, Q. M., and Wang, Q. W.: Contrasting effects of prolonged drought and nitrogen addition on growth and non-structural carbohydrate dynamics in coexisting Pinus koraiensis and Fraxinus mandshurica saplings, For. Res., 5, e003, https://doi.org/10.48130/forres-0025-0002, 2025.

Willard, S. J., Liang, G. P., Adkins, S., Foley, K., Murray, J., and Waring, B.: Land use drives the distribution of free, physically protected, and chemically protected soil organic carbon storage at a global scale, Glob. Change Biol., 30, https://doi.org/10.1111/gcb.17507, 2024.

Williams, A. and de Vries, F. T.: Plant root exudation under drought: implications for ecosystem functioning, New Phytol., 225, 1899–1905, https://doi.org/10.1111/nph.16223, 2020.

Wu, H., Peng, C., Moore, T. R., Hua, D., Li, C., Zhu, Q., Peichl, M., Arain, M. A., and Guo, Z.: Modeling dissolved organic carbon in temperate forest soils: TRIPLEX-DOC model development and validation, Geosci. Model Dev., 7, 867–881, https://doi.org/10.5194/gmd-7-867-2014, 2014.

Wu, J. F., Yao, H. X., Chen, X. H., and Chen, X. W.: Dynamics of dissolved organic carbon during drought and flood events: A phase-by-stages perspective, Sci. Total Environ., 871, https://doi.org/10.1016/j.scitotenv.2023.162158, 2023.

Wu, R. Q., Wang, Y. S., Huo, X. Y., Chen, W. J., and Wang, D. X.: Drought and vegetation restoration patterns shape soil enzyme activity and nutrient limitation dynamics in the loess plateau, J. Environ. Manage., 374. https://doi.org/10.1016/j.jenvman.2024.123846, 2025.

Wu, X. W., Luo, Y. Q., Weng, E. S., White, L., Ma, Y., and Zhou, X. H.: Conditional inversion to estimate parameters from eddy-flux observations, J. Plant Ecol., 2, 55–68, https://doi.org/10.1093/jpe/rtp005, 2009.

Xu, T., White, L., Hui, D. F., and Luo, Y. Q.: Probabilistic inversion of a terrestrial ecosystem model: Analysis of uncertainty in parameter estimation and model prediction, Global Biogeochem. Cy., 20, https://doi.org/10.1029/2005GB002468, 2006.

Yin, H., Zheng, H. W., Zhang, B., Tariq, A., Lv, G. H., Zeng, F. J., and Graciano, C.: Stoichiometry of C : N : P in the Roots of Alhagi sparsifolia Is More Sensitive to Soil Nutrients Than Aboveground Organs, Front. Plant Sci., 12, https://doi.org/10.3389/fpls.2021.698961, 2021.

Zhao, T. H., Yang, X., He, R., Shi, B. K., Gao, W. F., Ma, J. Y., and Sun, W.: Plant-soil microbe adaptive strategies reshape soil respiration components under multi-year precipitation frequency reduction and nitrogen addition in a semi-arid grassland, Funct. Ecol., 39, 2370–2380, https://doi.org/10.1111/1365-2435.70118, 2025.

Zhou, G. Y., Zhou, X. H., Liu, R. Q., Du, Z. G., Zhou, L. Y., Li, S. S., Liu, H. Y., Shao, J. J., Wang, J. W., Nie, Y. Y., Gao, J., Wang, M. H., Zhang, M. Y., Wang, X. H., and Bai, S. H.: Soil fungi and fine root biomass mediate drought-induced reductions in soil respiration, Funct. Ecol., 34, 2634–2643, https://doi.org/10.1111/1365-2435.13677, 2020.

Zhou, X. Q., Chen, C. R., Wang, Y. F., Xu, Z. H., Duan, J. C., Hao, Y. B., and Smaill, S.: Soil extractable carbon and nitrogen, microbial biomass and microbial metabolic activity in response to warming and increased precipitation in a semiarid Inner Mongolian grassland, Geoderma, 206, 24–31, https://doi.org/10.1016/j.geoderma.2013.04.020, 2013.